NeuroImage: Clinical 19 (2018) 160–166

Contents lists available at ScienceDirect

NeuroImage: Clinical

journal homepage: www.elsevier.com/locate/ynicl

Polymorphism in schizophrenia risk gene *MIR137* is associated with the posterior cingulate Cortex's activation and functional and structural connectivity in healthy controls

Zhifang Zhang[a,b], Tongjun Yan[c], Yanyan Wang[c], Qiumei Zhang[d,a,b], Wan Zhao[a,b], Xiongying Chen[a,b], Jinguo Zhai[d], Min Chen[d], Boqi Du[a,b], Xiaoxiang Deng[a,b], Feng Ji[d], Yutao Xiang[e,f], Hongjie Wu[g], Jie Song[g], Qi Dong[a,b], Chuansheng Chen[h], Jun Li[a,b,*]

[a] State Key Laboratory of Cognitive Neuroscience and Learning & IDG/McGovern Institute for Brain Research, Beijing Normal University, PR China
[b] Center for Collaboration and Innovation in Brain and Learning Sciences, Beijing Normal University, PR China
[c] The PLA 102nd Hospital and Mental Health Center of Military, Changzhou 213003, PR China
[d] School of Mental Health, Jining Medical University, 45# Jianshe South Road, Jining 272013, Shandong Province, PR China
[e] Beijing Anding Hospital, Beijing 100088, PR China
[f] Faculty of Health Sciences, University of Macau, Avenida da Universidade, Taipa, Macau
[g] Shengli Hospital of Shengli Petroleum Administration Bureau, Dongying 257022, Shandong Province, PR China
[h] Department of Psychology and Social Behavior, University of California, Irvine, CA 92697, United States

ARTICLE INFO

Keywords:
MIR137 gene
Working memory
Functional connectivity
Structural connectivity
Posterior cingulate cortex

ABSTRACT

MIR137 gene has been repeatedly reported as a schizophrenia risk gene in genome-wide association studies (GWAS). A polymorphism (rs1625579) at the *MIR137* gene has been associated with both neural activation and behavioral performance during a working memory task. This study examined *MIR137*'s associations with task-related (N-back working memory) fMRI, resting state fMRI, and diffusion tensor images (DTI) data in 177 healthy adults. We found less deactivation of the PCC in risk allele homozygotes (TT) as compared to the GT heterozygotes (cluster size = 630 voxels, cluster level $P_{FWE} < 0.001$) during the N-back task, which replicated previous findings. Using the identified cluster within the PCC as the seed, we further found decreased functional connectivity between the PCC and the anterior cingulate cortex and its adjacent medial prefrontal cortex (ACC/MPFC) in risk allele homozygotes during both resting state (cluster size = 427 voxels, cluster level $P_{FWE} = 0.001$) and the N-back task (cluster size = 73 voxels, cluster level $P_{FWE} = 0.05$). Finally, an analysis of our DTI data showed decreased white matter integrity of the posterior cingulum in risk allele homozygotes (cluster size = 214 voxels, cluster level $P_{FWE} = 0.03$). Taken together, rs1625579 seems to play an important role in both functional and structural connectivity between the PCC and the ACC/MPFC, which may serve as the brain mechanisms for the link between rs1625579 and schizophrenia.

1. Introduction

Schizophrenia is a complex mental illness with high heritability (Sullivan et al., 2003). Genome-wide association studies (GWAS) have repeatedly identified the *MIR137* gene (1p21.3) as one of the schizophrenia risk genes (Schizophrenia Psychiatric Genome-Wide Association Study, C, 2011; Schizophrenia Working Group of the Psychiatric Genomics, C, 2014). Rs1625579 is a single nucleotide polymorphism (SNP) within the *MIR137* gene which was first reported to show the strongest association with schizophrenia in European ancestry population (Schizophrenia Psychiatric Genome-Wide Association Study, C, 2011). A meta-analysis of the data from Han Chinese population has replicated this significant association (Zhang et al., 2016). The SNP rs1625579 has been associated with the expression of the putative primary transcript of the *MIR137* gene, microRNA-137 (miR-137) (Guella et al., 2013), which is a brain-enriched small RNA molecule that plays an important role in brain development (Silber et al., 2008; Smrt et al., 2010; Szulwach et al., 2010) and brain expression of various schizophrenia susceptibility genes (e.g. *TCF4*, *CACNA1C*, *CSMD1*, *C10orf26*, *ZNF804A, EFNB2*) (Guan et al., 2014; Kim et al., 2012; Kwon et al., 2013; Potkin et al., 2010; Schizophrenia Psychiatric Genome-Wide Association Study, C, 2011; Tooney, 2016). It is worth

* Corresponding author at: State Key Laboratory of Cognitive Neuroscience and Learning & IDG/McGovern Institute for Brain Research, Beijing Normal University, PR China.
E-mail address: lijundp@bnu.edu.cn (J. Li).

https://doi.org/10.1016/j.nicl.2018.03.039
Received 4 January 2018; Received in revised form 16 March 2018; Accepted 31 March 2018
Available online 03 April 2018

noting that a landmark GWAS of schizophrenia (Schizophrenia Working Group of the Psychiatric Genomics, C, 2014) has identified another SNP (rs1702294) within the same gene as the second most significant hit out of 128 SNPs that met genome-wide significance level, but rs1702294 is not polymorphic in Han Chinese.

The SNP rs1625579 has been linked to working memory, a core cognitive domain that is impaired in schizophrenia patients (Barch and Ceaser, 2012), in three independent studies (Cummings et al., 2013; Green et al., 2013; Ma et al., 2014). Risk allele homozygotes (TT) showed relatively worse working memory than the G allele carriers in both schizophrenia patients and healthy controls. Only one functional magnetic resonance imaging (fMRI) study has been conducted to examine relations between this SNP and brain functions (van Erp et al., 2014). Using Sternberg Item Recognition test to measure working memory, van Erp et al. (2014) found that the risk allele (T) was linked to altered activations at the posterior cingulate cortex (PCC) and the parahippocampal gyrus (a part of the hippocampus formation, HF), both of which are key nodes of the default mode network (DMN) (Raichle et al., 2001). In general, the DMN exhibits a high level of activity during resting state, but is suppressed when performing tasks with high cognitive demand (Greicius et al., 2003). The DMN's role in cognitive function (e.g. working memory) is likely due to its functional connections with other brain regions (Elton and Gao, 2015). Working-memory fMRI studies have found that poor working memory is linked to decreased functional connectivity both within the DMN (Hampson et al., 2006, 2010; Newton et al., 2011; Sambataro et al., 2010; Whitfield-Gabrieli and Ford, 2012) and between the DMN and the central executive network (CEN) (Leech et al., 2011; Newton et al., 2011; Sala-Llonch et al., 2012; Sambataro et al., 2010).

To replicate and extend van Erp et al.'s (2014) study, we collected genetic, task-related (N-back working memory) fMRI, resting state fMRI, and DTI data from 177 healthy Chinese adults. We hypothesized that the risk allele homozygotes would show less deactivation of the PCC and/or the HF. More importantly, we investigated the association between rs1625579 and functional connectivity of the PCC with the rest of the brain during both resting state and N-back task. We hypothesized that the risk allele homozygotes would show decreased functional connectivity between the PCC and the rest of the DMN and/or between the PCC and the CEN. Finally, because the cingulum tract is the main structural basis for functional connectivity between the PCC and the anterior cingulate cortex and its adjacent medial prefrontal cortex (ACC/MPFC) (Greicius et al., 2009), we examined the association between rs1625579 and the structure of this tract using diffusion tensor images (DTI) data. We hypothesized that the risk allele homozygotes would show disrupted white matter integrity within the cingulum tract.

2. Materials and methods

2.1. Subjects

A sample of 177 healthy Han Chinese adults (age range = 18 to 45 years; male to female gender ratio = 3:1) were recruited by advertisement. All subjects were interviewed by experienced psychiatrists to screen for any personal or family history of psychiatric disorders during an unstructured interview. All subjects had normal or corrected-to-normal vision and were right-handed as assessed by the Edinburgh handedness inventory. None of the subjects reported any history of hard drug use (e.g. cocaine, crack, heroin, methamphetamine, etc.). Due to their excessive head motion (> 3° or 3 mm), seven subjects were excluded from the N-back task data analysis and thirteen subjects were excluded from the resting state data analysis. All subjects were included in the DTI data analysis. It needs to be mentioned that, as reported in previous studies of Han Chinese (Wang et al., 2014; Yuan et al., 2015), the non-risk allele homozygotes (GG genotype) were also absent in the current sample. Of the 170 subjects included in the N-back task fMRI data analysis, 24 were heterozygotes (GT genotype) and 146 were risk allele homozygotes (TT genotype). The 164 subjects for the resting state fMRI data analysis included 22 heterozygotes and 142 risk allele homozygotes, and the 177 subjects for the DTI data analysis included 25 heterozygotes and 152 risk allele homozygotes. Detailed demographic information is presented in Table 1.

Table 1
Demographic factors and cognitive performance by rs1625579 genotype.

	Mean ± SD		T or χ^2	P
	GT	TT		
For the N-back task fMRI data				
N	24	146	–	–
Gender (male/female)	18/6	109/37	0.001	0.971
Age (years)	27.46 ± 5.20	26.90 ± 5.40	0.47	0.636
Education (years)	13.25 ± 3.00	13.31 ± 3.27	−0.09	0.932
IQ	116.33 ± 9.10	114.77 ± 11.34	0.64	0.523
2-Back (accuracy)	0.92 ± 0.08	0.88 ± 0.15	1.41	0.162
2-Back (RT)	363.49 ± 144.13	355.42 ± 111.65	0.31	0.754
For the resting-state fMRI data				
N	22	142	–	–
Gender (male/female)	16/6	104/38	0.003	0.960
Age (years)	27.82 ± 5.27	26.87 ± 5.43	0.77	0.443
Education (years)	13.41 ± 3.08	13.33 ± 3.28	0.10	0.920
IQ	116.64 ± 9.24	114.25 ± 11.54	0.92	0.357
For the DTI data				
N	25	152	–	–
Gender (male/female)	18/7	114/38	0.10	0.750
Age (years)	27.56 ± 5.12	26.95 ± 5.52	0.51	0.608
Education (years)	13.36 ± 2.98	13.38 ± 3.33	−0.04	0.972
IQ	116.52 ± 8.92	114.61 ± 11.46	0.79	0.429

RT: reaction time.

The protocol of this study was reviewed and approved by the Institutional Review Board of the Institute of Cognitive Neuroscience and Learning at Beijing Normal University. All subjects gave written informed consent for this study.

2.2. Genotyping

Genomic DNA was extracted using the standard method. The SNP rs1625579 (T > G) was genotyped using Taqman allele-specific assays on the 7900HT Fast Real-Time PCR System (Applied Biosystems, Foster City, CA, U.S.A.). PCR was performed in a 5 µl reaction volume which included 2.5 µl TaqMan™ Genotyping Master Mix, 0.125 µl TaqMan® SNP Genotyping Assays, 0.125 µl TE and 10 ng DNA. The thermal cycling conditions were 50 °C for 2 min, 95 °C for 10 min, 50 cycles of 92 °C for 15 s, and 60 °C for 1 min. The genotypes were identified using Sequence Detection System (SDS) Version 2.4 software (Applied Biosystems). The sample success rate for this SNP was 100%. The reproducibility of the genotyping was 100% based on a duplicate analysis of 40% of the genotypes.

2.3. fMRI task

The N-back task had been described in our previous studies (Yu et al., 2016; Zhang et al., 2015; Zhang et al., 2016). Briefly, the stimulus was a white circle presented randomly at one of the four corners of a grey diamond-shaped square. Subjects were required to make responses according to the current location of the white circle (0-back) or the location of the white circle seen 2 trials earlier (2-back). Responses were made by using a fiber-optic response box with four buttons that were also arranged in a diamond shape. Subjects pressed one of the four buttons to match the target stimulus. The task included two runs. Each run lasted 192 s and consisted of 8 blocks in which the 2-back condition alternated with the 0-back condition. A centrally placed fixation cross was presented for 16 s before each set of 4 blocks. Each block started

with a 4 s on-screen instruction (either the number "0" or "2" at the center of the screen indicating the type of working memory task to be performed). There were 8 trials in each block. In each trial (lasting for 2 s), the stimuli were presented for 500 ms, followed by a 1.5 s blank. All subjects received training before scan until their accuracy showed no more improvement. Accuracy and reaction time at the 2-back condition were used to reflect task performance.

2.4. Imaging data acquisition

Imaging data were all acquired at the Brain Imaging Center of Beijing Normal University. Subjects were scanned on a Siemens TIM Trio 3T scanner (Siemens, Erlangen, Germany) with their head snugly fixed with straps and foam pads to restrict head movement. Resting state images (240 volumes) were acquired first, followed by structural images scan. Then, subjects were moved out of the scanner and given training on the task. After the training, subjects went back into the scanner and were asked to perform the cognitive task while being scanned. Finally, two DTI scans were acquired. The resting state and task-related functional images were collected axially using the same echo-planar imaging (EPI) sequence: repetition time (TR) = 2000 ms; echo time (TE) = 30 ms; flip angle = 90°; field of view (FOV) = 200 × 200 mm^2; matrix size = 64 × 64; axial slices = 31; 4.0 mm slice thickness without gap (i.e. interleaved scan); voxel size = 3.1 × 3.1 × 4.0 mm^3. Structural images were acquired using a T1-weighted sagittal 3D magnetization-prepared rapid gradient echo (MPRAGE) sequence: TR = 2530 ms; TE = 3.45 ms; flip angle = 7°; FOV = 256 × 256 mm^2; matrix size = 256 × 256; slices = 176; thickness = 1.0 mm; voxel size = 1 × 1 × 1 mm^3. DTI data were acquired using a spin-echo single-shot EPI sequence: 75 slices; 2.0 mm thickness; TR = 10,000 ms; TE = 91 ms; FOV = 256 × 256 mm; matrix size = 128 × 128; 30 directions with a b-value = 1000 s/mm^2 and an additional image without diffusion weighting (b-value = 0 s/mm^2).

2.5. Task-related fMRI data preprocessing

Task-related fMRI data were preprocessed using Statistical Parametric Mapping (SPM12b, Wellcome Department of Cognitive Neurology, London, UK). Preprocessing included realignment (all subsequent images generated in each run of a certain subject were realigned to the first image and any subject with > 3 mm translation or 3° rotation would be excluded), normalization to Montreal Neurological Institute (MNI) space (normalization parameters from subjects' native space to MNI space was generated by SPM12's unified segmentation of their T1 image, coregistered to their T1 images, and normalized to the MNI space), re-sampling to voxel size of 3 × 3 × 3 mm^3, and spatial smoothing with 8 mm full-width at half maximum (FWHM) of the Gaussian kernel. Contrast image (2 back vs. 0 back) for each subject was produced in first-level analysis. In this analysis, a high-pass filter at 128 s was used to remove noise associated with low-frequency confounds. The resulting contrast images were then entered into the second-level analysis.

Preprocessing for the functional connectivity analysis on the same task fMRI data was implemented on SPM12b. The cluster showing significant genotype effect in the above brain activation analysis was used as the seed. Following our previous study (Zhang et al., 2016), we first extracted the first eigenvariate from the seed. The first eigenvariate represents the weighted mean of the ROI data that results in time series with maximum possible variance (Bedenbender et al., 2011; Penny et al., 2011; Esslinger et al., 2009; King et al., 2015; Mothersill et al., 2014; Muller et al., 2013). Then, correlation coefficients between the seed and all other voxels were estimated after regressing out the task time series, white matter signals, cerebral spinal fluid signals, and six head movement parameters. A high-pass filter of 128 s was used. The generated functional connectivity maps were entered into the group-level analysis.

2.6. Resting state fMRI data preprocessing

Resting state fMRI data were preprocessed in DPABI version 2.3 (http://rfmri.org/dpabia, a key component of The R-fMRI Maps Project under The Human Brain Data Sharing Initiative) (Yan et al., 2016). Following van den Heuvel et al.'s (2017) suggestion, our preprocessing included the following steps: removing the first 10 time points, realignment, normalization to the MNI space (T1 images were used), resampling to voxel size of 3 × 3 × 3 mm^3, smoothing (FWHM = 8 mm), detrending, band-pass filtering (0.01–0.1 Hz), and nuisance covariates regression (the white matter, the cerebral spinal fluid, the global mean signals and the head motion effect, Friston 24-parameter model, Friston et al., 1996). In addition, Power et al.'s (2012) "scrubbing" method was used to remove residual motion artifact. For this method, framewise displacement Jenkinson type was used, and the threshold for "bad" time points was set at 0.5. One time point before and two time points after the "bad" time point were scrubbed using the cut (delete) method. It should be mentioned that because all of our subjects' mean framewise displacement Jenkinson values were < 0.5, all subjects were included in the resting state functional connectivity analysis. The seed was the same as that used in the task-related functional connectivity analysis mentioned above. Pearson correlation coefficients between time courses of the seed and whole-brain voxels were used to construct the functional connectivity maps, which were then converted to *Z*-score maps using Fisher *r*-to-*Z* transformation. The Z-score maps were entered into the group-level analysis.

2.7. DTI data preprocessing

Processing of our DTI data was implemented using a pipeline toolbox – PANDA (http://www.nitrc.org/projects/panda) (Cui et al., 2013). The preprocessing included the following steps: converting DICOM files into NIfTI images (using MRIcron's *dcm2nii* tool), estimating the brain mask (using b0 image and FSL's *bet* command), cropping the raw images (using *fslroi* command, with the cropping gap = 3 mm), correcting the eddy current distortion and motion artifacts (using *flirt* command), averaging 2 sets of diffusion images (using *fslmaths*), voxel-wise calculation of multiple tensor-based metrics in subjects' native space (using *dtifit* command to calculate fractional anisotropy (FA), which reflects white matter integrity), normalization (using *fnirt* and *applywarp* commands to normalize FA to the MNI space and to resample to voxel size of 2 × 2 × 2 mm^3), and smoothing (using *fslmaths* command with Gaussian kernel = 6 mm). The resulting FA images were entered into the group-level analysis.

2.8. Data analysis

The Hardy-Weinberg test of the SNP was done by using the PLINK program (Purcell et al., 2007). Demographic factors including age, gender, IQ, and years of education and cognitive performance among genotypic groups were compared using either two-sample *t*-test or chi-square test (two-tailed).

In the group-level analysis of N-back task fMRI, resting state fMRI, and DTI data, two-sample t-test was used to compare differences between the two genotype groups (GT vs. TT) controlling for subjects' age, gender, and years of education. For the activation analysis of the N-back task fMRI data and the functional connectivity analysis of the resting state fMRI data, significance level was set at uncorrected voxel-level threshold of $P < 0.005$ combined with whole-brain FWE corrected cluster-level threshold of $P < 0.05$. For the functional connectivity analysis of the N-back task fMRI data, the group-level analysis was limited to anterior cingulate cortex/medial prefrontal cortex (ACC/MPFC, bilateral ACC + medial superior frontal cortex, using the AAL template in the WFU PickAtlas software, http://fmri.wfubmc.edu/software/PickAtlas). Significance level for this analysis was set at uncorrected voxel-level threshold of $P < 0.005$ combined with small-

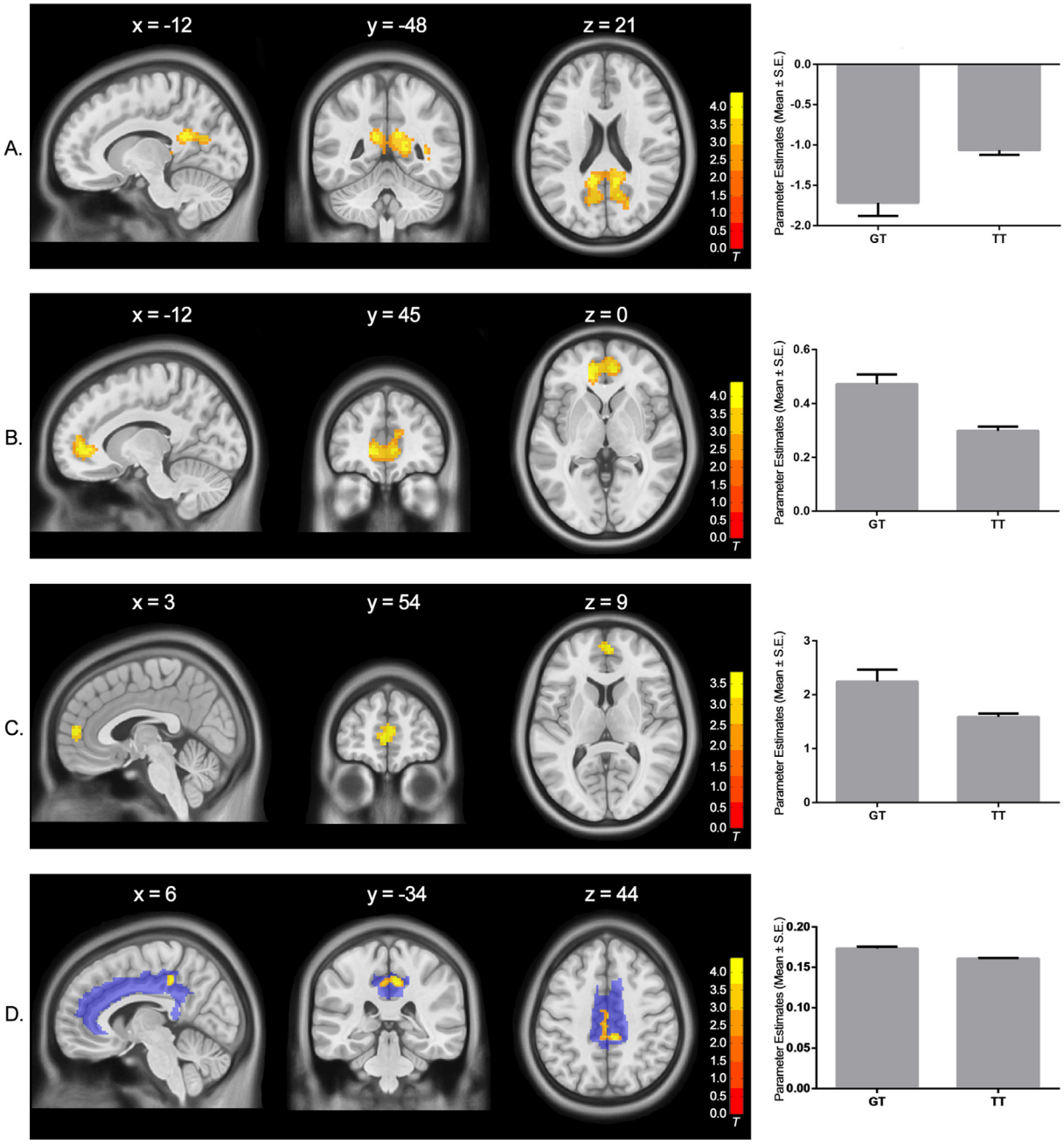

Fig. 1. Significant association between *MIR137* gene polymorphism (rs1625579) and the PCC's neural activation and connectivity. Panel A: Risk allele homozygotes (TT) showed less deactivation at the PCC when performing the N-back working memory task (cluster size = 630 voxels, whole-brain FWE corrected $P < 0.001$; peak MNI coordinates: x = −12, y = −48, z = 21, $T = 4.41$). Panel B: Risk allele homozygotes showed reduced functional connectivity between the PCC and the ACC/MPFC during resting state (cluster size = 427 voxels, whole-brain FWE corrected $P = 0.001$; peak MNI coordinates: x = −12, y = 45, z = 0, $T = 4.42$). Panel C: Risk allele homozygotes also showed decreased functional connectivity between PCC and ACC/MPFC when performing the N-back task (cluster size = 73 voxels, small-volume FWE corrected $P = 0.05$; peak MNI coordinates: x = 3, y = 54, z = 9, $T = 3.79$). Panel D: Risk allele homozygotes showed reduced FA at the posterior cingulum (cluster size = 214 voxels, small-volume FWE corrected $P = 0.03$; peak MNI coordinates: x = 6, y = −34, z = 44, $T = 4.29$). The transparent blue area in panel D showed the cingulum tract mask used in the analysis.

volume FWE corrected cluster-level threshold of $P < 0.05$. For the analysis of the DTI data, we limited our group-level analysis within the cingulum tract (the union of the anterior, middle and posterior cingulum tract). Significance level was also set at uncorrected voxel-level threshold of $P < 0.005$ combined with small-volume FWE corrected cluster-level threshold of $P < 0.05$.

3. Results

No deviation from Hardy-Weinberg Equilibrium was found. The two genotype groups were comparable on all demographic factors and cognitive task performance (all *P*-values > 0.05). (See Table 1).

Our whole-brain analysis of the N-back task fMRI data found a significant genotype effect at the PCC (cluster size = 630 voxels, cluster level $P_{FWE} < 0.001$; peak MNI coordinates: x = −12, y = −48, z = 21, $T = 4.41$). The risk allele homozygotes (TT) showed less deactivation compared with the GT genotype (See Fig. 1A). No significant effect was found when images of the GT group were subtracted from those of the TT group. No significant genotype effect was found at the hippocampus formation.

Using the significant cluster at the PCC as the seed, we explored possible functional dysconnectivity that may be associated with rs1625579. Our result showed that, as compared to the GT group, the TT group showed decreased resting state functional connectivity from the PCC to the anterior cingulate cortex and its adjacent medial prefrontal cortex (ACC/MPFC) (cluster size = 427 voxels, cluster level $P_{FWE} = 0.001$; peak MNI coordinates: x = −12, y = 45, z = 0, $T = 4.42$; See Fig. 1B). The same pattern was found for the N-back task (cluster size = 73 voxels, cluster level $P_{FWE} = 0.05$; peak MNI coordinates: x = 3, y = 54, z = 9, $T = 3.79$; See Fig. 1C) when we restricted our analysis within the ACC/MPFC.

When we restricted our analysis on DTI data within the cingulum, our results showed that, compared to the GT genotype, the risk allele homozygotes (TT) showed significantly decreased FA value (i.e. decreased white matter integrity) at the posterior cingulum (cluster size = 214 voxels, cluster level $P_{FWE} = 0.03$; peak MNI coordinates: x = 6, y = −34, z = 44, $T = 4.29$; See Fig. 1D).

Finally, we found significant associations between the accuracy on the 2-back task and the level of the PCC's activity during the working memory task ($r = -0.32$, $P < 0.001$, see Supplementary Fig. S1A), between the level of the PCC's activity and the functional connectivity seeded from the PCC to the ACC/MPFC during the working memory task ($r = -0.30$, $P < 0.001$, see Supplementary Fig. S1B), and between the functional connectivity seeded from the PCC to the ACC/MPFC and the mean FA within the posterior cingulum (for resting state, $r = 0.33$, $P < 0.001$, see Supplementary Fig. S1C; for the working memory task, $r = 0.18$, $P = 0.020$, see Supplementary Fig. S1D).

4. Discussion

This study examined the effects of the *MIR137* rs1625579 genotype on neural correlates of working memory. Consistent with van Erp et al.'s (2014) fMRI study, we found that the risk allele homozygotes (TT) exhibited altered activation (less deactivation) at the PCC as compared to the GT heterozygotes during working memory. Less deactivation at the PCC when performing working memory tasks has been found in schizophrenia patients (Bittner et al., 2015; Fryer et al., 2013; Haatveit et al., 2016; Kim et al., 2009; Wu et al., 2014) and has been linked to poorer working memory performance (Eryilmaz et al., 2016; Pu et al., 2016; Zhou et al., 2016), which was replicated in the current study (See Supplementary Fig. S1). The PCC is a major node of the DMN (Raichle, 2015), which is activated at rest or when performing tasks that are directed inward (e.g. autobiographical memory), but is suppressed when performing external goal-directed tasks (e.g. working memory) (Elton and Gao, 2015). Efficient DMN suppression has been regarded as a sign of successfully re-configuring brain resources to focus on external goal-directed behavior while ignoring task-irrelevant stimuli (Raichle et al., 2001; Whitfield-Gabrieli et al., 2009; Yaakub et al., 2013). The less deactivation at the PCC found for the TT group seemed to indicate that subjects with two copies of the risk allele were less efficient in reconfiguring brain resources to meet the needs of the working memory task.

The current study extended van Erp et al.'s finding (van Erp et al., 2014) by discovering decreased functional connectivity between the PCC and the ACC/MPFC in risk allele homozygotes during both resting state and working memory performance. This result is consistent with a previous finding that miR-137 could alter presynaptic plasticity (for example, miR-137 could affect the expressions of some presynaptic target genes such as the presynaptic target genes complexin-1 (Cplx1) and synaptotagmin-1 (Syt1), leading to altered vesicle release), which is critical for functional connectivity (Siegert et al., 2015). In the DMN, the ACC/MPFC was the second major node next to the PCC (Buckner et al., 2008). The functional connectivity of the two nodes is supposed to maintain normal baseline brain function (via synchronous activation at resting state) (De Luca et al., 2006; Greicius et al., 2003; Laufs et al., 2003; Margulies et al., 2009; Raichle et al., 2001; Uddin et al., 2009) and to facilitate cognitive processing such as working memory (via synchronous suppression) (Fransson, 2006; Greicius et al., 2003; Huang et al., 2016; Kim et al., 2009; Sala-Llonch et al., 2012; Tomasi et al., 2006). However, schizophrenia patients have been found to have decreased functional connectivity of the above two nodes during both resting state (Bluhm et al., 2007; Camchong et al., 2011; Lynall et al., 2010; Rotarska-Jagiela et al., 2010) and working memory performance (Fryer et al., 2013; Haatveit et al., 2016; Pu et al., 2016; Wu et al., 2014; Zhang et al., 2013; Zhou et al., 2016). This decreased functional connectivity probably indicates inefficient communication and poor synchronous activity between the above nodes, which helps to explain how rs1625579 contributes to the etiology of schizophrenia.

We further found that the decreased functional connectivity between the PCC and the ACC/MPFC as discussed above may have a structural basis. Anatomically, the PCC and the ACC/MPFC were connected by the cingulum tract (Greicius et al., 2009). Functional connectivity between the PCC and the ACC/MPFC during resting state has been reported to be positively correlated with the average FA value of the cingulum tract (van den Heuvel et al., 2008), which was replicated in this study (See Supplementary Fig. S1). As for the posterior part of the cingulum specifically, a lower FA has been found for schizophrenia patients (Fujiwara et al., 2007; Mitelman et al., 2006; Roalf et al., 2015; Schneiderman et al., 2009; Segal et al., 2010; Sun et al., 2015) and linked to worse working memory (Karlsgodt et al., 2008; Nestor et al., 2008). As a result, it is possible that the disruption of the posterior cingulum in the risk allele homozygotes of rs1625569 may further decrease the functional connectivity strength between the PCC and the ACC/MPFC and contribute to working memory deficit in schizophrenia.

5. Conclusions

In conclusion, this study replicated van Erp et al.'s (2014) finding of less deactivation at the PCC for the rs1625579 risk allele homozygotes during working memory, and found that the risk allele was also significantly associated with decreased functional (during both working memory and resting state) and structural connectivity between the PCC and the ACC/MPFC. These results deepened our understanding of the brain mechanisms for the association between rs1625579 and schizophrenia and also point to the importance of considering the central role of the DMN in this association.

Supplementary data to this article can be found online at https://doi.org/10.1016/j.nicl.2018.03.039.

Acknowledgements

We would like to thank all the healthy volunteers. This work was supported by grants from the National Key Basic Research Program of China (2014CB846103), the Natural Science Foundation of China (81571045), and the Provincial Natural Science Foundation, China (ZR2017LH036). The authors declare no conflict of interest.

Author contributions

Li J, Dong Q and Chen CS designed the study and wrote the protocol. Zhang ZF and Yan TJ managed the literature searches and analyses. Zhang ZF, Yan TJ, Wang YY, Zhang QM, Zhao W, Chen XY, Zhai JG, Chen M, Du BQ, Deng XX, Ji F, Xiang YT, Wu HJ, and Song J selected and evaluated the sample of healthy controls. Zhang ZF undertook the statistical analysis. Zhang ZF, Li J and Chen CS wrote the first draft of the manuscript. All authors contributed to and have approved the final manuscript.

Financial disclosures

Authors declare no competing financial interests in relation with this manuscript.

References

Barch, D.M., Ceaser, A., 2012. Cognition in schizophrenia: core psychological and neural mechanisms. Trends Cogn. Sci. 16, 27–34.

Bedenbender, J., Paulus, F.M., Krach, S., Pyka, M., Sommer, J., Krug, A., Witt, S.H., Rietschel, M., Laneri, D., Kircher, T., Jansen, A., 2011. Functional connectivity analyses in imaging genetics: considerations on methods and data interpretation. PLoS One 6, e26354.

Bittner, R.A., Linden, D.E.J., Roebroeck, A., Hartling, F., Rotarska-Jagiela, A., Maurer, K., Goebel, R., Singer, W., Haenschel, C., 2015. The when and where of working memory dysfunction in early-onset schizophrenia-a functional magnetic resonance imaging study. Cereb. Cortex 25, 2494–2506.

Bluhm, R.L., Miller, J., Lanius, R.A., Osuch, E.A., Boksman, K., Neufeld, R.W., Theberge, J., Schaefer, B., Williamson, P., 2007. Spontaneous low-frequency fluctuations in the BOLD signal in schizophrenic patients: anomalies in the default network. Schizophr. Bull. 33, 1004–1012.

Buckner, R.L., Andrews-Hanna, J.R., Schacter, D.L., 2008. The brain's default network: anatomy, function, and relevance to disease. Ann. N. Y. Acad. Sci. 1124, 1–38.

Camchong, J., MacDonald 3rd, A.W., Bell, C., Mueller, B.A., Lim, K.O., 2011. Altered functional and anatomical connectivity in schizophrenia. Schizophr. Bull. 37, 640–650.

Cui, Z., Zhong, S., Xu, P., He, Y., Gong, G., 2013. PANDA: a pipeline toolbox for analyzing brain diffusion images. Front. Hum. Neurosci. 7, 42.

Cummings, E., Donohoe, G., Hargreaves, A., Moore, S., Fahey, C., Dinan, T.G., McDonald, C., O'Callaghan, E., O'Neill, F.A., Waddington, J.L., Murphy, K.C., Morris, D.W., Gill, M., Corvin, A., 2013. Mood congruent psychotic symptoms and specific cognitive deficits in carriers of the novel schizophrenia risk variant at MIR-137. Neurosci. Lett. 532, 33–38.

De Luca, M., Beckmann, C.F., De Stefano, N., Matthews, P.M., Smith, S.M., 2006. fMRI resting state networks define distinct modes of long-distance interactions in the human brain. NeuroImage 29, 1359–1367.

Elton, A., Gao, W., 2015. Task-positive functional connectivity of the default mode network transcends task domain. J. Cogn. Neurosci. 27, 2369–2381.

Eryilmaz, H., Tanner, A.S., Ho, N.F., Nitenson, A.Z., Silverstein, N.J., Petruzzi, L.J., Goff, D.C., Manoach, D.S., Roffman, J.L., 2016. Disrupted working memory circuitry in schizophrenia: disentangling fMRI markers of core pathology vs other aspects of impaired performance. Neuropsychopharmacology 41, 2411–2420.

Esslinger, C., Walter, H., Kirsch, P., Erk, S., Schnell, K., Arnold, C., Haddad, L., Mier, D., Opitz von Boberfeld, C., Raab, K., Witt, S.H., Rietschel, M., Cichon, S., Meyer-Lindenberg, A., 2009. Neural mechanisms of a genome-wide supported psychosis variant. Science 324, 605.

Fransson, P., 2006. How default is the default mode of brain function? Further evidence from intrinsic BOLD signal fluctuations. Neuropsychologia 44, 2836–2845.

Friston, K.J., Williams, S., Howard, R., Frackowiak, R.S., Turner, R., 1996. Movement-related effects in fMRI time-series. Magn. Reson. Med. 35, 346–355.

Fryer, S.L., Woods, S.W., Kiehl, K.A., Calhoun, V.D., Pearlson, G.D., Roach, B.J., Ford, J.M., Srihari, V.H., McGlashan, T.H., Mathalon, D.H., 2013. Deficient suppression of default mode regions during working memory in individuals with early psychosis and at clinical high-risk for psychosis. Front. Psych. 4, 92.

Fujiwara, H., Namiki, C., Hirao, K., Miyata, J., Shimizu, M., Fukuyama, H., Sawamoto, N., Hayashi, T., Murai, T., 2007. Anterior and posterior cingulum abnormalities and their association with psychopathology in schizophrenia: a diffusion tensor imaging study. Schizophr. Res. 95, 215–222.

Green, M.J., Cairns, M.J., Wu, J., Dragovic, M., Jablensky, A., Tooney, P.A., Scott, R.J., Carr, V.J., Australian Schizophrenia Research, B., 2013. Genome-wide supported variant MIR137 and severe negative symptoms predict membership of an impaired cognitive subtype of schizophrenia. Mol. Psychiatry 18, 774–780.

Greicius, M.D., Krasnow, B., Reiss, A.L., Menon, V., 2003. Functional connectivity in the resting brain: a network analysis of the default mode hypothesis. Proc. Natl. Acad. Sci. U. S. A. 100, 253–258.

Greicius, M.D., Supekar, K., Menon, V., Dougherty, R.F., 2009. Resting-state functional connectivity reflects structural connectivity in the default mode network. Cereb. Cortex 19, 72–78.

Guan, F., Zhang, B., Yan, T., Li, L., Liu, F., Li, T., Feng, Z., Zhang, B., Liu, X., Li, S., 2014. MIR137 gene and target gene CACNA1C of miR-137 contribute to schizophrenia susceptibility in Han Chinese. Schizophr. Res. 152, 97–104.

Guella, I., Sequeira, A., Rollins, B., Morgan, L., Torri, F., van Erp, T.G., Myers, R.M., Barchas, J.D., Schatzberg, A.F., Watson, S.J., Akil, H., Bunney, W.E., Potkin, S.G., Macciardi, F., Vawter, M.P., 2013. Analysis of miR-137 expression and rs1625579 in dorsolateral prefrontal cortex. J. Psychiatr. Res. 47, 1215–1221.

Haatveit, B., Jensen, J., Alnaes, D., Kaufmann, T., Brandt, C.L., Thoresen, C., Andreassen, O.A., Melle, I., Ueland, T., Westlye, L.T., 2016. Reduced load-dependent default mode network deactivation across executive tasks in schizophrenia spectrum disorders. Neuroimage Clin 12, 389–396.

Hampson, M., Driesen, N., Roth, J.K., Gore, J.C., Constable, R.T., 2010. Functional connectivity between task-positive and task-negative brain areas and its relation to working memory performance. Magn. Reson. Imaging 28, 1051–1057.

Hampson, M., Driesen, N.R., Skudlarski, P., Gore, J.C., Constable, R.T., 2006. Brain connectivity related to working memory performance. J. Neurosci. 26, 13338–13343.

Huang, A.S., Klein, D.N., Leung, H.C., 2016. Load-related brain activation predicts spatial working memory performance in youth aged 9–12 and is associated with executive function at earlier ages. Dev. Cogn. Neurosci.-Neth 17, 1–9.

Karlsgodt, K.H., van Erp, T.G., Poldrack, R.A., Bearden, C.E., Nuechterlein, K.H., Cannon, T.D., 2008. Diffusion tensor imaging of the superior longitudinal fasciculus and working memory in recent-onset schizophrenia. Biol. Psychiatry 63, 512–518.

Kim, A.H., Parker, E.K., Williamson, V., McMichael, G.O., Fanous, A.H., Vladimirov, V.I., 2012. Experimental validation of candidate schizophrenia gene ZNF804A as target for hsa-miR-137. Schizophr. Res. 141, 60–64.

Kim, D.I., Manoach, D.S., Mathalon, D.H., Turner, J.A., Mannell, M., Brown, G.G., Ford, J.M., Gollub, R.L., White, T., Wible, C., Belger, A., Bockholt, H.J., Clark, V.P., Lauriello, J., O'Leary, D., Mueller, B.A., Lim, K.O., Andreasen, N., Potkin, S.G., Calhoun, V.D., 2009. Dysregulation of working memory and default-mode networks in schizophrenia using independent component analysis, an fBIRN and MCIC study. Hum. Brain Mapp. 30, 3795–3811.

King, D.R., de Chastelaine, M., Elward, R.L., Wang, T.H., Rugg, M.D., 2015. Recollection-related increases in functional connectivity predict individual differences in memory accuracy. J. Neurosci. 35, 1763–1772.

Kwon, E., Wang, W., Tsai, L.H., 2013. Validation of schizophrenia-associated genes CSMD1, C10orf26, CACNA1C and TCF4 as miR-137 targets. Mol. Psychiatry 18, 11–12.

Laufs, H., Krakow, K., Sterzer, P., Eger, E., Beyerle, A., Salek-Haddadi, A., Kleinschmidt, A., 2003. Electroencephalographic signatures of attentional and cognitive default modes in spontaneous brain activity fluctuations at rest. Proc. Natl. Acad. Sci. U. S. A. 100, 11053–11058.

Leech, R., Kamourieh, S., Beckmann, C.F., Sharp, D.J., 2011. Fractionating the default mode network: distinct contributions of the ventral and dorsal posterior cingulate cortex to cognitive control. J. Neurosci. 31, 3217–3224.

Lynall, M.E., Bassett, D.S., Kerwin, R., McKenna, P.J., Kitzbichler, M., Muller, U., Bullmore, E., 2010. Functional connectivity and brain networks in schizophrenia. J. Neurosci. 30, 9477–9487.

Ma, G., Yin, J., Fu, J., Luo, X., Zhou, H., Tao, H., Cui, L., Li, Y., Lin, Z., Zhao, B., Li, Z., Lin, J., Li, K., 2014. Association of a miRNA-137 polymorphism with schizophrenia in a Southern Chinese Han population. Biomed. Res. Int. 2014, 751267.

Margulies, D.S., Vincent, J.L., Kelly, C., Lohmann, G., Uddin, L.Q., Biswal, B.B., Villringer, A., Castellanos, F.X., Milham, M.P., Petrides, M., 2009. Precuneus shares intrinsic functional architecture in humans and monkeys. Proc. Natl. Acad. Sci. U. S. A. 106, 20069–20074.

Mitelman, S.A., Newmark, R.E., Torosjan, Y., Chu, K.W., Brickman, A.M., Haznedar, M.M., Hazlett, E.A., Tang, C.Y., Shihabuddin, L., Buchsbaum, M.S., 2006. White matter fractional anisotropy and outcome in schizophrenia. Schizophr. Res. 87, 138–159.

Mothersill, O., Morris, D.W., Kelly, S., Rose, E.J., Fahey, C., O'Brien, C., Lyne, R., Reilly, R., Gill, M., Corvin, A.P., Donohoe, G., 2014. Effects of MIR137 on fronto-amygdala functional connectivity. NeuroImage 90, 189–195.

Muller, V.I., Cieslik, E.C., Laird, A.R., Fox, P.T., Eickhoff, S.B., 2013. Dysregulated left inferior parietal activity in schizophrenia and depression: functional connectivity and characterization. Front. Hum. Neurosci. 7, 268.

Nestor, P.G., Kubicki, M., Niznikiewicz, M., Gurrera, R.J., McCarley, R.W., Shenton, M.E., 2008. Neuropsychological disturbance in schizophrenia: a diffusion tensor imaging study. Neuropsychology 22, 246–254.

Newton, A.T., Morgan, V.L., Rogers, B.P., Gore, J.C., 2011. Modulation of steady state functional connectivity in the default mode and working memory networks by cognitive load. Hum. Brain Mapp. 32, 1649–1659.

Penny, W.D.F., Friston, K., Ashburner, J.T., Kiebel, S.J., Nichols, T.E., 2011. Statistical Parametric Mapping: The Analysis of Functional Brain Images. pp. 656.

Potkin, S.G., Macciardi, F., Guffanti, G., Fallon, J.H., Wang, Q., Turner, J.A., Lakatos, A., Miles, M.F., Lander, A., Vawter, M.P., Xie, X., 2010. Identifying gene regulatory networks in schizophrenia. NeuroImage 53, 839–847.

Power, J.D., Barnes, K.A., Snyder, A.Z., Schlaggar, B.L., Petersen, S.E., 2012. Spurious but systematic correlations in functional connectivity MRI networks arise from subject motion. NeuroImage 59, 2142–2154.

Pu, W., Luo, Q., Palaniyappan, L., Xue, Z., Yao, S., Feng, J., Liu, Z., 2016. Failed co-operative, but not competitive, interaction between large-scale brain networks impairs working memory in schizophrenia. Psychol. Med. 46, 1211–1224.

Purcell, S., Neale, B., Todd-Brown, K., Thomas, L., Ferreira, M.A., Bender, D., Maller, J., Sklar, P., de Bakker, P.I., Daly, M.J., Sham, P.C., 2007. PLINK: a tool set for whole-genome association and population-based linkage analyses. Am. J. Hum. Genet. 81, 559–575.

Raichle, M.E., 2015. The brain's default mode network. Annu. Rev. Neurosci. 38, 433–447.

Raichle, M.E., MacLeod, A.M., Snyder, A.Z., Powers, W.J., Gusnard, D.A., Shulman, G.L., 2001. A default mode of brain function. Proc. Natl. Acad. Sci. U. S. A. 98, 676–682.

Roalf, D.R., Gur, R.E., Verma, R., Parker, W.A., Quarmley, M., Ruparel, K., Gur, R.C., 2015. White matter microstructure in schizophrenia: associations to neurocognition and clinical symptomatology. Schizophr. Res. 161, 42–49.

Rotarska-Jagiela, A., van de Ven, V., Oertel-Knochel, V., Uhlhaas, P.J., Vogeley, K., Linden, D.E., 2010. Resting-state functional network correlates of psychotic symptoms in schizophrenia. Schizophr. Res. 117, 21–30.

Sala-Llonch, R., Pena-Gomez, C., Arenaza-Urquijo, E.M., Vidal-Pineiro, D., Bargallo, N., Junque, C., Bartres-Faz, D., 2012. Brain connectivity during resting state and subsequent working memory task predicts behavioural performance. Cortex 48, 1187–1196.

Sambataro, F., Murty, V.P., Callicott, J.H., Tan, H.Y., Das, S., Weinberger, D.R., Mattay, V.S., 2010. Age-related alterations in default mode network: impact on working memory performance. Neurobiol. Aging 31, 839–852.

Schizophrenia Psychiatric Genome-Wide Association Study, C, 2011. Genome-wide association study identifies five new schizophrenia loci. Nat. Genet. 43, 969–976.

Schizophrenia Working Group of the Psychiatric Genomics, C, 2014. Biological insights from 108 schizophrenia-associated genetic loci. Nature 511, 421–427.

Schneiderman, J.S., Buchsbaum, M.S., Haznedar, M.M., Hazlett, E.A., Brickman, A.M., Shihabuddin, L., Brand, J.G., Torosjan, Y., Newmark, R.E., Canfield, E.L., Tang, C.,

Aronowitz, J., Paul-Odouard, R., Hof, P.R., 2009. Age and diffusion tensor anisotropy in adolescent and adult patients with schizophrenia. NeuroImage 45, 662–671.
Segal, D., Haznedar, M.M., Hazlett, E.A., Entis, J.J., Newmark, R.E., Torosjan, Y., Schneiderman, J.S., Friedman, J., Chu, K.W., Tang, C.Y., Buchsbaum, M.S., Hof, P.R., 2010. Diffusion tensor anisotropy in the cingulate gyrus in schizophrenia. NeuroImage 50, 357–365.
Siegert, S., Seo, J., Kwon, E.J., Rudenko, A., Cho, S., Wang, W., Flood, Z., Martorell, A.J., Ericsson, M., Mungenast, A.E., Tsai, L.H., 2015. The schizophrenia risk gene product miR-137 alters presynaptic plasticity. Nat. Neurosci. 18, 1008–1016.
Silber, J., Lim, D.A., Petritsch, C., Persson, A.I., Maunakea, A.K., Yu, M., Vandenberg, S.R., Ginzinger, D.G., James, C.D., Costello, J.F., Bergers, G., Weiss, W.A., Alvarez-Buylla, A., Hodgson, J.G., 2008. miR-124 and miR-137 inhibit proliferation of glioblastoma multiforme cells and induce differentiation of brain tumor stem cells. BMC Med. 6, 14.
Smrt, R.D., Szulwach, K.E., Pfeiffer, R.L., Li, X., Guo, W., Pathania, M., Teng, Z.Q., Luo, Y., Peng, J., Bordey, A., Jin, P., Zhao, X., 2010. MicroRNA miR-137 regulates neuronal maturation by targeting ubiquitin ligase mind bomb-1. Stem Cells 28, 1060–1070.
Sullivan, P.F., Kendler, K.S., Neale, M.C., 2003. Schizophrenia as a complex trait: evidence from a meta-analysis of twin studies. Arch. Gen. Psychiatry 60, 1187–1192.
Sun, H., Lui, S., Yao, L., Deng, W., Xiao, Y., Zhang, W., Huang, X., Hu, J., Bi, F., Li, T., Sweeney, J.A., Gong, Q., 2015. Two patterns of white matter abnormalities in medication-naive patients with first-episode schizophrenia revealed by diffusion tensor imaging and cluster analysis. JAMA Psychiat. 72, 678–686.
Szulwach, K.E., Li, X., Smrt, R.D., Li, Y., Luo, Y., Lin, L., Santistevan, N.J., Li, W., Zhao, X., Jin, P., 2010. Cross talk between microRNA and epigenetic regulation in adult neurogenesis. J. Cell Biol. 189, 127–141.
Tomasi, D., Ernst, T., Caparelli, E.C., Chang, L., 2006. Common deactivation patterns during working memory and visual attention tasks: an intra-subject fMRI study at 4 Tesla. Hum. Brain Mapp. 27, 694–705.
Tooney, P.A., 2016. Attention: schizophrenia risk gene product miR-137 now targeting EFNB2. EBioMedicine 12, 10–11.
Uddin, L.Q., Kelly, A.M., Biswal, B.B., Castellanos, F.X., Milham, M.P., 2009. Functional connectivity of default mode network components: correlation, anticorrelation, and causality. Hum. Brain Mapp. 30, 625–637.
van den Heuvel, M., Mandl, R., Luigjes, J., Hulshoff Pol, H., 2008. Microstructural organization of the cingulum tract and the level of default mode functional connectivity. J. Neurosci. 28, 10844–10851.
van den Heuvel, M.P., de Lange, S.C., Zalesky, A., Seguin, C., Yeo, B.T.T., Schmidt, R., 2017. Proportional thresholding in resting-state fMRI functional connectivity networks and consequences for patient-control connectome studies: issues and recommendations. NeuroImage 152, 437–449.
van Erp, T.G., Guella, I., Vawter, M.P., Turner, J., Brown, G.G., McCarthy, G., Greve, D.N., Glover, G.H., Calhoun, V.D., Lim, K.O., Bustillo, J.R., Belger, A., Ford, J.M., Mathalon, D.H., Diaz, M., Preda, A., Nguyen, D., Macciardi, F., Potkin, S.G., 2014. Schizophrenia miR-137 locus risk genotype is associated with dorsolateral prefrontal cortex hyperactivation. Biol. Psychiatry 75, 398–405.
Wang, S., Li, W., Zhang, H., Wang, X., Yang, G., Zhao, J., Yang, Y., Lv, L., 2014. Association of microRNA137 gene polymorphisms with age at onset and positive symptoms of schizophrenia in a Han Chinese population. Int. J. Psychiatry Med. 47, 153–168.
Whitfield-Gabrieli, S., Ford, J.M., 2012. Default mode network activity and connectivity in psychopathology. Annu. Rev. Clin. Psychol. 8, 49–76.
Whitfield-Gabrieli, S., Thermenos, H.W., Milanovic, S., Tsuang, M.T., Faraone, S.V., McCarley, R.W., Shenton, M.E., Green, A.I., Nieto-Castanon, A., LaViolette, P., Wojcik, J., Gabrieli, J.D., Seidman, L.J., 2009. Hyperactivity and hyperconnectivity of the default network in schizophrenia and in first-degree relatives of persons with schizophrenia. Proc. Natl. Acad. Sci. U. S. A. 106, 1279–1284.
Wu, G., Wang, Y., Mwansisya, T.E., Pu, W., Zhang, H., Liu, C., Yang, Q., Chen, E.Y., Xue, Z., Liu, Z., Shan, B., 2014. Effective connectivity of the posterior cingulate and medial prefrontal cortices relates to working memory impairment in schizophrenic and bipolar patients. Schizophr. Res. 158, 85–90.
Yaakub, S.N., Dorairaj, K., Poh, J.S., Asplund, C.L., Krishnan, R., Lee, J., Keefe, R.S.E., Adcock, R.A., Wood, S.J., Chee, M.W.L., 2013. Preserved working memory and altered brain activation in persons at risk for psychosis. Am. J. Psychiatry 170, 1297–1307.
Yan, C.G., Wang, X.D., Zuo, X.N., Zang, Y.F., 2016. DPABI: data processing & analysis for (resting-state) brain imaging. Neuroinformatics 14, 339–351.
Yu, P., Chen, X., Zhao, W., Zhang, Z., Zhang, Q., Han, B., Zhai, J., Chen, M., Du, B., Deng, X., Ji, F., Wang, C., Xiang, Y.T., Li, D., Wu, H., Li, J., Dong, Q., Chen, C., 2016. Effect of rs1063843 in the CAMKK2 gene on the dorsolateral prefrontal cortex. Hum. Brain Mapp. 37, 2398–2406.
Yuan, J.M., Cheng, Z.H., Zhang, F.Q., Zhou, Z.H., Yu, S., Jin, C.H., 2015. Lack of association between microRNA-137 SNP rs1625579 and schizophrenia in a replication study of Han Chinese. Mol. Gen. Genomics. 290, 297–301.
Zhang, H.R., Wei, X.M., Tao, H.J., Mwansisya, T.E., Pu, W.D., He, Z., Hu, A.M., Xu, L., Liu, Z.N., Shan, B.C., Xue, Z.M., 2013. Opposite effective connectivity in the posterior cingulate and medial prefrontal cortex between first-episode schizophrenic patients with suicide risk and healthy controls. PLoS One 8.
Zhang, P., Bian, Y., Liu, N., Tang, Y., Pan, C., Hu, Y., Tang, Z., 2016. The SNP rs1625579 in miR-137 gene and risk of schizophrenia in Chinese population: a meta-analysis. Compr. Psychiatry 67, 26–32.
Zhang, Z., Chen, X., Yu, P., Zhang, Q., Sun, X., Gu, H., Zhang, H., Zhai, J., Chen, M., Du, B., Deng, X., Ji, F., Wang, C., Xiang, Y., Li, D., Wu, H., Li, J., Dong, Q., Chen, C., 2015. Evidence for the contribution of NOS1 gene polymorphism (rs3782206) to prefrontal function in schizophrenia patients and healthy controls. Neuropsychopharmacology 40, 1383–1394.
Zhang, Z., Chen, X., Yu, P., Zhang, Q., Sun, X., Gu, H., Zhang, H., Zhai, J., Chen, M., Du, B., Deng, X., Ji, F., Wang, C., Xiang, Y., Li, D., Wu, H., Li, J., Dong, Q., Chen, C., 2016. Effect of rs1344706 in the ZNF804A gene on the connectivity between the hippocampal formation and posterior cingulate cortex. Schizophr. Res. 170, 48–54.
Zhou, L., Pu, W., Wang, J., Liu, H., Wu, G., Liu, C., Mwansisya, T.E., Tao, H., Chen, X., Huang, X., Lv, D., Xue, Z., Shan, B., Liu, Z., 2016. Inefficient DMN suppression in schizophrenia patients with impaired cognitive function but not patients with preserved cognitive function. Sci. Rep. 6, 21657.